POLYPUBLIE
Polytechnique Montréal

POLYTECHNIQUE MONTRÉAL
UNIVERSITÉ D'INGÉNIERIE

Document en libre accès dans PolyPublie
Open Access document in PolyPublie

Document publié chez l'éditeur officiel
Document issued by the official publisher

Multi-gas detection using Fabry-Perot interferometers on silicon chip

Régis Guertin, Marc-Antoine Bianki, Cédric Lemieux-Leduc, Yves-Alain Peter

[a]*Department of Engineering Physics, Polytechnique Montréal, Montréal, QC, Canada*

Abstract

This work presents an all optical on chip integrated gas sensor array for sensing multiple gas simultaneously using non-specific polymers as the sensing material. The individual sensors are vertically etched into silicon. They are made of two Bragg mirrors forming a Fabry-Perot cavity which is functionalized with different polymers such as polyethylene glycol (PEG), SU-8 and polydimethylsiloxane (PDMS). Multi-gas detection was achieved for various gas mixtures of isopropyl alcohol (IPA), H_2O, valeric acid and butanol. Using a linear model, we report limits of detection as low as 8.1 parts per million (ppm) for valeric acid within mixtures.

Key words: Gas sensing, Fabry-Perot, Polymer, Non-specific detection

1 Introduction

The industry is continuously looking for new gas sensors offering improved performance in discriminating different types of volatile organic compound (VOC) while being insensitive to humidity and temperature. However, current technologies have crosstalk between gases and are sensitive to temperature [1,2,3]. The present trend in modern gas sensing is to have a sensor specific to a particular gas thus preventing crosstalk. These types of sensors require highly selective elements for specific analytes, which are extremely rare if any. However, new kinds of sensor arrays are emerging, with sensing elements that are not specific individually but provide specificity when operated in parallel [4,5].

Optical noses are being developed for multi-gas sensing and selectivity is hard to achieve [6,7]. A promising category of sensing elements are polymers. They are sensitive to many VOCs and have demonstrated diversified sensitivity for several VOCs and polymer combinations [8,9,10]. This work demonstrates an optical nose based on Fabry-Perot cavities vertically etched in silicon by anisotropic plasma etching initially proposed by St-Gelais et al. [8]. Functionalisation of the sensor is

achieved by filling the cavity with a polymer, swelling when exposed to a gas. The expansion is inducing a variation in the cavity length and is thus shifting the resonance frequency of the Fabry-Perot cavity. Selectivity of Fabry-Perot sensors were demonstrated in Jubinville et al. [9], using different polymers leading to the fabrication of a polymer sensor array. In this work, different polymer responses are used simultaneously to identify gas mixtures using a cross sensitive sensor for multi-gas detection. The proposed sensor targets gas emitted by industries such as wastewater treatment plants and solid waste management.

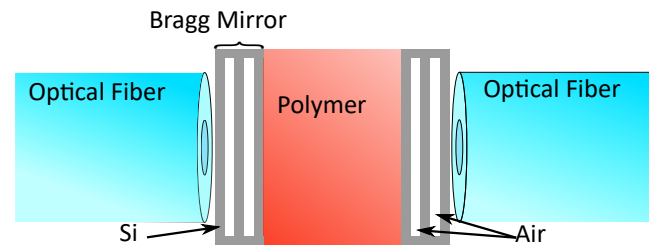## 2 Material and Methods

2.1 Fabrication Process

Fig. 1. Design of the sensor with two Bragg mirrors forming a Fabry-Perot cavity.

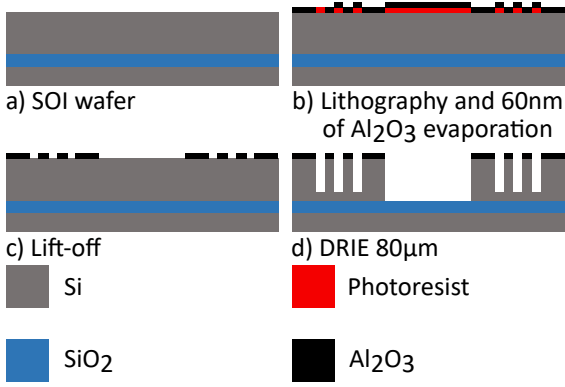The design presented in Fig. 1 is composed of two Bragg mirrors with alternating silicon and air layers forming a

Fig. 2. Fabrication Process

Fabry-Perot cavity, with dimensions of $2.79\mu m$, $3.5\mu m$ respectively and a cavity length of $72\mu m$. These dimensions follow the design parameters presented in St-Gelais et al. [11]. The cavity is filled with a polymer using a microfluidic channel and reservoir. There are also two U grooves helping the alignment of the fibers in and out of the cavity. The fabrication process starts with a silicon on insulator (SOI) wafer as shown in Fig. 2. The device layer is $80\mu m$ thick. An etching mask of 60 nm Al_2O_3 is then evaporated with electron beam and patterned with lift-off. The features are etched using Deep Reactive Ion Etching (DRIE) with SF_6 and C_4F_8. Due to the ARDE effect [12], the SiO_2 layer of the SOI is used as an etch stop layer. Since the width of the U grooves is larger than the width of the layers of the Bragg mirrors, they etch faster.

Polymers are injected into the cavity with a syringe and flow thanks to capillarity into the microfluidic channel. The polymers used in this study are PDMS (Sylgard 184) from Dow Corning, PEG from Sigma Aldrich (mol wt 200), and SU-8 2000.5 from Microchem. Only three of the eight cavities are filled with the presented polymers.

For easier handling, fibers are held in U grooves with UV curing optical glue (*NOA61*) and placed on a polylactic acid (PLA) sample holder as presented in Fig. 3.

2.2 Experimental Setup

The experimental setup shown in Fig. 4 was designed to inject three different gas using a bubbler with the carrier gas going through the liquids [13]. Nitrogen is used as a carrier gas, a dilution gas and also for referencing. The gas mixture is diluted and mixed inside the confinement box. To minimize the transition time from a reference to the gas mixture of interest, a pneumatic valve was installed inside the chamber. It directs the analytes onto the sample or into the exhaust. Three mass flow controllers (*MKS 1179C*) are used to regulate the gas. The mass flow controller 1 ranges from 0 to 10 sLm (standard Liters per minute) and is used for dilution. The two others are used to inject carrier gas. The mass flow 2 controls the nitrogen flow from 0 to 20 sccm (standard cubic centimeters per minute) and the mass flow 3 from 0 to 50 sccm. To orient the flow directly on the sensor and minimize the dead volumes, a small enclosure in PLA was built. A temperature sensitivity of $0.1\,\mathrm{nm\,K^{-1}}$ has been previously reported due to the thermo-optic coefficient and thermal expansion coefficient of the polymer [9]. In consequence, the temperature was kept constant at room temperature.
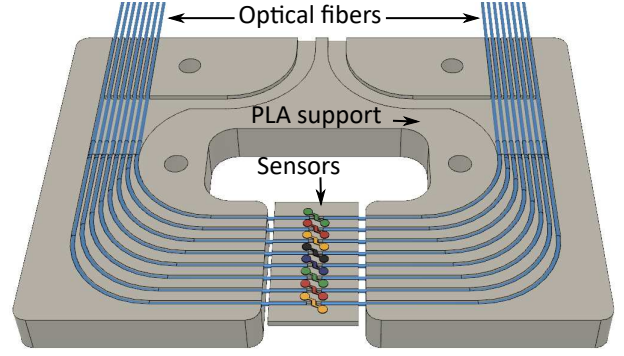

Fig. 3. Assembly of the sensor on a PLA plate with the sensors in the middle. Eight fibers are leaving the chip on each side.

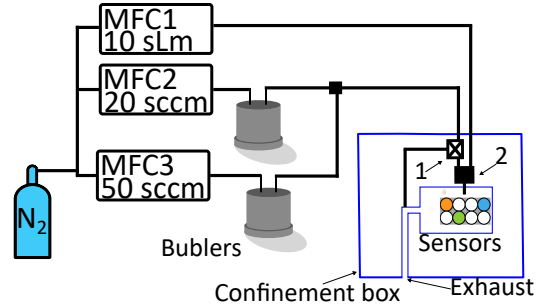Fig. 4. Gas exposure experimental setup. 1-Pneumatic Valve. 2-Mixer.

The optical setup is composed of an *Agilent 81960A* tunable laser whose signal is divided with a planar lightwave circuit (PLC) from *Fiber Solution*. The signals go to the sensors and are collected by 4 photodiodes (*N4477A*). Using four $2x1$ optical switches from *Fiber Solution*, eight cavities can be measured simultaneously. The setup has an acquisition rate of 0.5 Hz.

3 Experiment

Three different mixtures were measured at constant temperature. The combinations are H_2O-IPA, butanol-IPA and butanol-valeric acid. Fig. 6 presents the shift of the Fabry-Perot resonances with different concentrations of IPA and H_2O with the three polymers. Fig. 5 shows an optical spectrum of an SU-8 filled cavity exposed to nitrogen and a mixture of IPA and H_2O. A detailed optical analysis is presented in St-Gelais et al. [8]. Each Fabry-

Perot resonance was recorded applying second order regression to remove noise. The variation in wavelength was measured using a differential method [3]. The baseline was subtracted from the sensor response between each exposure to a gas mixture. The dynamic range is limited by the LOD (limit of detection) up to the maximum concentration injected by the gas injection setup. The upper limit of the dynamic range is fundamentally limited by the saturation of the polymer and the deformation capacity of the cavity.
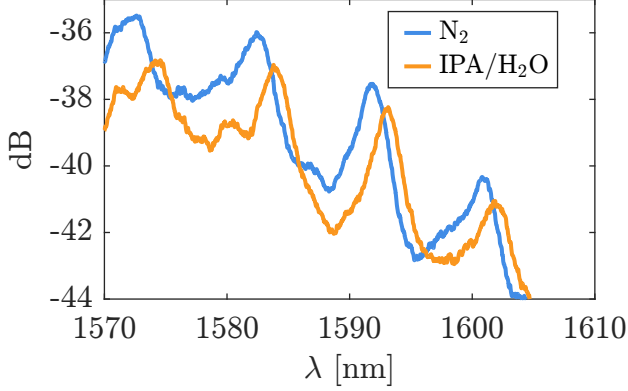

Fig. 5. Transmission spectrum of the FP cavity filled with SU-8 while exposed to N_2 and a mixture of IPA and H_2O. Resonances shift from the original position due to swelling and refractive index change. Similar effect is observed with cavities filled with different polymers.
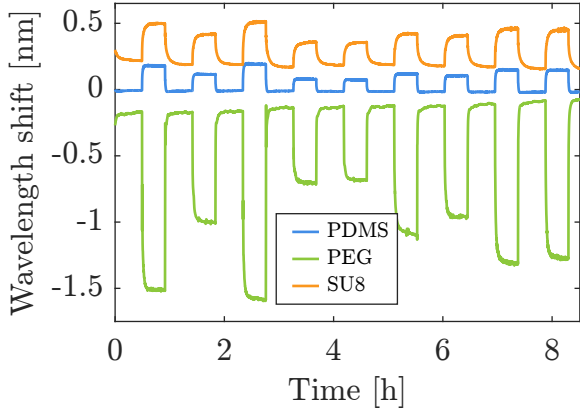

Fig. 6. Wavelength shift of the resonance peak for different sensors functionalized with different polymers upon exposure to a mixture of IPA and H_2O. In orange, the sensor is filled with SU-8, in blue with PDMS and in green with PEG.

From Fig. 6, one can see that the sensor is stable over time. However, the PEG sensor exhibits a little drift.

3.1 Sensitivity of the sensors

The sensitivity S was calculated using the following equation (1)

$$S = \frac{\Delta\lambda}{\Delta C_n} \tag{1}$$

where $\Delta\lambda$ is the shift in the resonance peak wavelength and ΔC_n is the change of gas concentration. In the case of a multi-gas detection, the sensitivity must be rewritten as the matrix $\hat{S}$ calculated with a multi-variable linear regression, as described in Carey et al. [14], taking the following form

$$\hat{S} = (C^T C)^{-1} C^T \Lambda, \tag{2}$$

where $\Lambda = (\Lambda_{SU_8}, \Lambda_{PDMS}, \Lambda_{PEG}, ...)$ is the measured wavelength shift of multiple sensors and $C = (C_{gas_A}, C_{gas_B}, ...)$ the concentrations of multiple gas sources. The wavelength shift of the sensors can then be predicted with $\hat{\Lambda}$ in equation (3):

$$\hat{\Lambda} = C\hat{S}. \tag{3}$$

Upon exposure to IPA and H_2O simultaneously, the response of each individual sensor provides a linear response as shown in Fig. 7, where the lines are drawn with a slope going through the origin.

On these graphs, a good correlation is obtained from a linear model. For PDMS, PEG and SU-8, a R^2 of 0.89, 0.99 and 0.89 respectively is calculated confirming the applicability of the linear model. Also, from this simple model, there is no noticeable interaction between two gas. The same conclusion is observed for the other mixtures.

From equation (2), the sensitivity of each polymer towards different gas can be obtained and are shown in Table 1. Sensitivities depend on the partition coefficient K_{PA} [11] and the polymer/gas couple solubility [15]. PEG's sensitivities are negative leading to a contraction of the polymer upon exposure to theses gas. The two other are swelling given the positive sensitivity. The collinearity of the sensitivity of each gas $\hat{S}_n$ can be cal-

Table 1
Sensitivity $\hat{S}$ table. All values are in nm ppm^{-1}

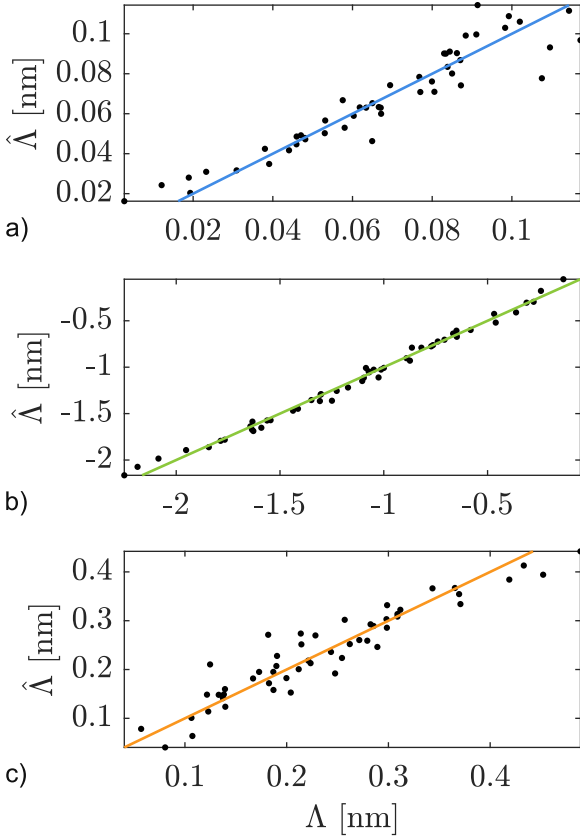|	PEG	SU-8	PDMS
IPA	-4.1×10^{-4}	6.8×10^{-5}	2.0×10^{-5}
Butanol	-1.3×10^{-3}	6.6×10^{-4}	1.7×10^{-4}
Valeric Acid	-4.4×10^{-2}	3.1×10^{-3}	2.8×10^{-3}
H_2O	-6.5×10^{-4}	2.0×10^{-4}	5.0×10^{-5}

Fig. 7. Linear models to predict the shift of the sensors using different concentration values of IPA and H_2O ranging from 0 ppm to 4260 ppm and 0 ppm to 945 ppm respectively. a) PDMS b) PEG c) SU-8

culated using equation (4) where $R_{n,m}$ is the angle between the sensitivity vector of two different gas.

$$R_{n,m} = \arccos\left(\frac{\left\langle \hat{S_n}, \hat{S_m} \right\rangle}{||\hat{S_n}|| \, ||\hat{S_m}||}\right) \tag{4}$$

155　The angles are displayed in Table 2. Low collinearity leads to a high discrimination and is noted by an angle close to 90° leading to a high differentiation of gas in a mixture.

Table 2
Selectivity angle between two gases. Values not in parentheses are direct measurements.

	IPA	Butanol	Valeric Acid	H_2O
IPA	N/A	17.9^o	(25.2^o)	7.7^o
Butanol	17.9^o	N/A	(8.5^o)	(10.2^o)
Valeric Acid	(25.2^o)	8.5	N/A	(17.6^o)
H_2O	7.7^o	(10.2^o)	(17.6^o)	N/A

Angles range from 7.7^o to 25.6^o confirming the possibil-
160　ity to differentiate the components of a mixture.

3.2　Gas identification

The predicting parameter $\hat{\kappa}$ allows to predict the concentration of a gas mixture knowing (5)

$$\hat{\kappa} = (\Lambda^T \Lambda)^{-1} \Lambda^T C \tag{5}$$

165　and the predicted concentrations $\hat{C}$ are then calculated using (6)

$$\hat{C} = \Lambda \hat{\kappa}. \tag{6}$$

Equation (6) provides the relation between the measured wavelength shift upon any concentration of gas using a
170　linear model. To identify the concentration of each gas, equation (6) is used and the results are plotted in Fig. 8 for a mixture of different concentrations of IPA and H_2O.

Figure 8 reports the predicted values of a mixture of
175　IPA and H_2O using the linear model. Figure 8a shows a good correlation with a R^2 of 0.94 from the predicted and injected concentration of IPA. The predicted values give an overall error E of 9.9% (see Table 3). However,

Table 3
Gas identification in pair for three different mixtures. The mean error μ and standard deviation σ are presented.

Mixtures	1	2	3
Gas 1	IPA	Butanol	Butanol
(μ,σ)ppm	(269,343)	(49,63)	(58,67)
E(%)	9.9%	31%	28%
Gas 2	H_2O	IPA	Valeric Acid
(μ,σ)ppm	(163,200)	(342,433)	(2.1,2.7)
E(%)	28%	13%	29%

for H_2O (Fig. 8b), the sensors exhibit a R^2 of 0.51, with
180　an overall error of 28%. The sensor is able to distinguish IPA with a good accuracy in the presence of any concentration of H_2O.

The LOD can be calculated using three times the standard deviation σ on the prediction error of the concen-
185　tration in a mixture of gas. Limits of detection could have been calculated using the ratio of noise over sensitivity, but in a case of a multi-gas detection, this would underestimate the error and not represent real-world applications. Table 4 presents the LOD of the sensors for
190　different gas. The LOD for measurements with a single gas is in the ppm range. However, in the presence of a second gas, the precision is less and the LOD increases by an order of magnitude on each gas. This is explained
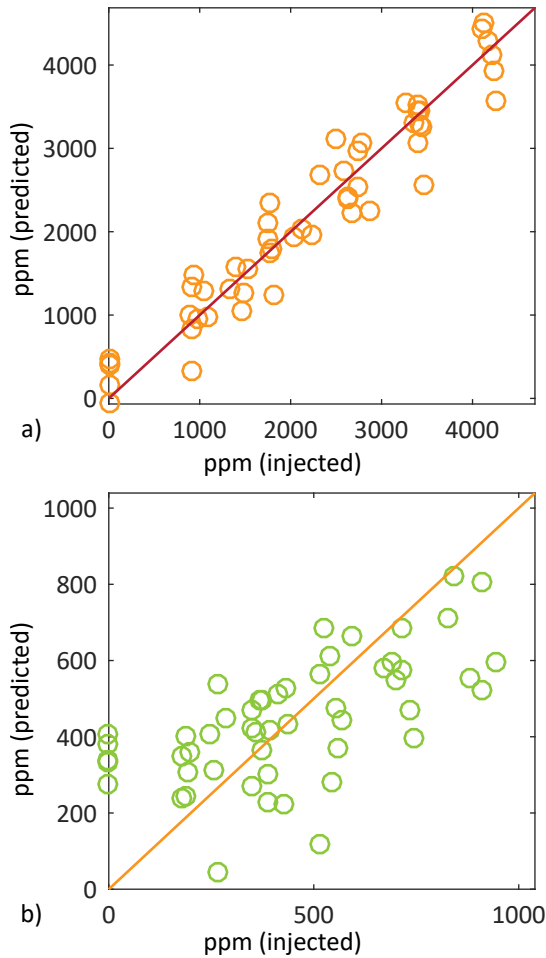
Fig. 8. Injected concentration versus predicted concentration $\hat{C}$ of a mixture of IPA and H_2O. a) Injected concentrations of IPA ranging from 0 ppm to 4100ppm. b) Injected concentrations of H_2O ranging from 0 ppm to 945 ppm

Table 4
Limit of detection comparison for single gas and multi-gas detection. Values are in ppm.

Gas	LOD (with N_2)	LOD (Mixture)
IPA	28	1029
H2O	13.5	600
Butanol	14.3	189
Valeric Acid	0.27	8.1

by the low selectivity of the sensor and a maximum measured selectivity of 17.9^o. Even in a mixture of gas, LOD as low as 8.1ppm was achieved for valeric acid. An angle closer to 90° could probably be achieved with dedicated polymers and would decrease drastically the ambiguity added in a gas mixture.

4 Conclusion

In this work, we demonstrated the possibility to measure different mixtures of two gas simultaneously with an all optical Fabry-Perot gas sensor functionalized with three different polymers (PDMS, PEG and SU-8). The analysis of the mixtures was achieved with a non-specific detector able to reach limits of detection as low as 8.1ppm in the case of valeric acid. Higher differentiation of mixtures could be achieved using dedicated polymers. Using a larger number of sensitive element could also lead to higher performance.

References

[1] S. Khan, S. L. Calvé, D. Newport, A review of optical interferometry techniques for VOC detection, Sensors and Actuators A: Physical 302 (2020) 111782.

[2] H. Nazemi, A. Joseph, J. Park, A. Emadi, Advanced micro- and nano-gas sensor technology: A review, Sensors 19 (6) (2019) 1285.

[3] K. Arshak, E. Moore, G. Lyons, J. Harris, S. Clifford, A review of gas sensors employed in electronic nose applications, Sensor review 24 (2) (2004) 181–198.

[4] K. J. Johnson, S. L. Rose-Pehrsson, Sensor array design for complex sensing tasks, Annual Review of Analytical Chemistry 8 (1) (2015) 287–310.

[5] K. J. Albert, N. S. Lewis, C. L. Schauer, G. A. Sotzing, S. E. Stitzel, T. P. Vaid, D. R. Walt, Cross-reactive chemical sensor arrays, Chemical Reviews 100 (7) (2000) 2595–2626.

[6] S. Brenet, A. John-Herpin, F.-X. Gallat, B. Musnier, A. Buhot, C. Herrier, T. Rousselle, T. Livache, Y. Hou, Highly-selective optoelectronic nose based on surface plasmonresonance imaging for sensing volatile organic compounds, Analytical Chemistry.

[7] M. J. Aernecke, D. R. Walt, Optical-fiber arrays for vapor sensing, Sensors and Actuators B: Chemical 142 (2) (2009) 464–469.

[8] R. St-Gelais, G. Mackey, J. Saunders, J. Zhou, A. Leblanc-Hotte, A. Poulin, J. A. Barnes, H.-P. Loock, R. S. Brown, Y.-A. Peter, Gas sensing using polymer-functionalized deformable fabry–perot interferometers, Sensors and Actuators B: Chemical 182 (2013) 45–52.

[9] P. Jubinville, R. Guertin, L. Erbilgin, W. Skene, Y.-A. Peter, Selective in-plane fabry-pérot gas sensor functionalized with polymer, in: IEEE/LEOS International Conference on Optical MEMS and Nanophotonics, Santa Fe, NW, 2017.

[10] M. Benetti, D. Cannatà, E. Verona, A. P. Papavlu, V. C. Dinca, T. Lippert, M. Dinescu, F. D. Pietrantonio, Highly selective surface acoustic wave e-nose implemented by laser direct writing, Sensors and Actuators B: Chemical 283 (2019) 154–162.

[11] R. St-Gelais, A. Poulin, Y.-A. Peter, Advances in modeling, design, and fabrication of deep-etched multilayer resonators, Journal of Lightwave Technology 30 (12) (2012) 1900–1908.

[12] B. Wu, A. Kumar, S. Pamarthy, High aspect ratio silicon etch: A review, Journal of Applied Physics 108 (5) (2010) 051101.

[13] H. Boer, Mass flow controlled evaporation system, Le Journal de Physique IV 5 (C5) (1995) C5–961.

[14] W. P. Carey, K. R. Beebe, B. R. Kowalski, Multicomponent analysis using an array of piezoelectric crystal sensors, Analytical chemistry 59 (11) (1987) 1529–1534.

[15] J. Feller, Y. Grohens, Evolution of electrical properties of some conductive polymer composite textiles with organic solvent vapours diffusion, Sensors and Actuators B: Chemical 97 (2-3) (2004) 231–242.

260